Jabirian
Journal of Biointerface Research in Pharmaceutics and Applied Chemistry
ISSN: 2584-2536 (Online)
Vol.3(1), Mar 2026, pp, 1-7
Journal homepage: https://sprinpub.com/jabirian

Research Article

Facile One-Pot Synthesis of Imidazole (MID): A Highly Sensitive Turn-Off Fluorescence Probe for Mercury (II) ion Detection

Md. Zafer Alam [1], *Salman A. Khan* [2*]

Department of Chemistry, School of Sciences, Maulana Azad National Urdu University, Hyderabad 500032, Telangana, India

ARTICLE INFO

Keywords:
Fluorescent sensor; Mercury (II) ion detection; Imidazole; one-pot synthesis; Turn-off Fluorescence; Metal ion sensing

Article History:
Received: 23-01-2026
Revised: 22-02-2026
Accepted: 01-03-2026
Published: 16-03-2026

ABSTRACT

A new highly fluorescence and sensitive fluorescent probe 4-(1-(4-methoxyphenyl)-4,5-diphenyl-1H-imidazol-2-yl)-N,N-diphenylaniline (MID) was prepared for the monitoring the mercury (II) ions with fluorometric behaviour in environmental samples. A significant fluorescence quenching was observed with MID in association with Hg2+ ions. MID can detect quiet low concentration of Hg2+ ions. The structure of MID was confirmed by 1H-NMR, 13C-NMR and mass spectrometry. However, the association of and complexation of MID with Hg2+ ions analysed by Job's plot titration and graph, the results revealed 2:1 ratio of MID with Hg2+ ions. Furthermore, the probe MID respond rapidly, and shows promising candidate for the selective recognition of Hg2+ ions in real samples.

Introduction

Mercury ion is the one of most hazardous heavy metal pollutants widely present in agriculture systems, soil environments and industrial wastewater. Mercury contamination create a serious threat to human health and ecosystems because even at low concentration in vapour state it can cause severe toxic effects. Exposure to mercury can lead to different health diseases including a well-known Minamata disease, Kidney damage, various neurological disorder, since it easily enter in biological membranes and accumulate in living organisms [1]. Mercury compounds are used in various industries including coal combustion, gold mining, caustic soda manufacturing, and oil refining [2], which significantly contributes to environmental contamination. Therefore, the selective and sensitive detection of mercury ion in trace amount in both biological as well as environmental models is of great importance [3].

There different analytical methods have been utilised to identify the Hg2+ in the samples, such as X-ray fluorescence spectrometry [4], high- performance liquid chromatography (HPLC), Liquid chromatography [5], atomic absorption chromatography [6], mass spectrometry [7], ion chromatography [8], and gas chromatography [9]. However, these methods displayed high accuracy and reliability, they often require sophisticated instrumentation, costly operation, preparation of complex sample. While, the fluorescence-based sensing techniques have gained considerable attention because of their rapid response, low cost, suitable for real-time analysis, high selectivity and sensitivity, ease to control of the analytes in complex samples.

Among the reported various fluorescent sensing systems, heterocyclic compounds have been widely used because of their tunable electronic structures and strong metal-ion coordination ability. Imidazole is a pent-acyclic hetero-aromatic ring containing two N-atoms at non-adjacent position (1 and 3) within the ring. Its molecular formula C3H4N2, and it exhibits a planar structure with aromatic character due to the delocalization of six π-electrons across the ring. Imidazole represents an important heterocyclic scaffold in organic and medicinal chemistry, owing to its versatile chemical reactivity and significant biological relevance. Naturally occurring imidazole derivatives play crucial roles in biological system; for instance, the amino acid histidine and the biologically active molecule histamine both contain imidazole rings. Additionally, the imidazole moiety is a key component in the active sites of many enzymes, particularly those containing heme groups, where it coordinates to metal ions such as iron. Imidazole exhibits amphoteric behaviour, acting as both a weak base and a weak acid. The nitrogen at position 1 (N-1) typically participates in protonation or coordination with metal ions, making imidazole a valuable ligand in coordination chemistry. Imidazole derivatives have attracted significant interest due to their diverse applications in pharmaceuticals, agrochemicals, corrosion inhibitors, ionic liquids, and as scaffolds in the design of fluorescent sensors, as well as anticancer, antimicrobial, and anti-inflammatory agents. Among these, azo-imidazole derivatives represent an important class of compounds under active scientific investigation. Due to their intense coloration, they have long been utilized as dyes and pigments, and have applications in drugs, cosmetics, and biological activities including antibacterial, anticancer effects [10].

Because of the advantages of the fluorescent chemosensor method, in this research article we synthesized an imidazole derivative (MID) via a facile one-pot procedure and investigated its application as a highly sensitive turn-off fluorescent sensor for the selective and specific identification of Hg2+ ions. The

* *Corresponding Author*:
Email: daniszafferalam@gmail.com (*Z. Alom*)
https://doi.org/10.55559/jjbrpac.v3i1.623

obtained derivative (MID) displays efficient fluorescence quenching in the presence of mercury ions, demonstrating its application for the identification of mercury contamination in biological and environmental samples.

Experiment

2.1 Chemicals, equipments, and instruments

All the chemicals and starting used for the preparation of MID including Benzil, ammonium-acetate, N,N-diphenyl benzaldehyde were procured from reputable commercial suppliers such as Sigma-Aldrich and Merck. These chemicals were employed without any further purification. Solvents used for both synthetic procedures and spectroscopic investigations were of analytical grade and required no additional treatment. Stock solutions of the imidazole-based derivatives were prepared in acetonitrile. All synthetic operations were performed in conventional laboratory glassware under standard ambient conditions. To assess the selectivity and binding affinity of the synthesized IMI-derivatives for toxic metal ion sensing, a broad spectrum of metal cations was examined. These included Na+, Ag+, Mg2+, Ca2+, Mn2+, Fe2+, Co2+, Cu2+, Zn2+, Pb2+, Cd2+, Hg2+, Fe3+, Al3+, and Ce4+ ions. All metal salts were prepared in deionized water to ensure high purity and consistency of the solutions. Initial verification of the synthesized compounds was performed via thin-layer chromatography (TLC) using silica gel 60 F254 plates. Melting point were recorded with a microprocessor-controlled apparatus (RLE-241-H). Structural elucidation was conducted using FT-IR (Bruker Tensor 37), 1H and 13C NMR spectroscopy (Bruker AVANCE, 400–500 MHz for 1H and 75–126 MHz for 13C, using $CDCl_3$-d_6), and mass spectrometry (Bruker Compass Data Analysis v4.2). Photo-physical properties were investigated using UV-Vis absorption spectroscopy with SYSTRONICS UV-Vis double-beam spectrophotometer (2206TS) and fluorescence emission spectroscopy with a PerkinElmer FL6500 fluorimeter.

2.2 Synthesis of 4-(1-(4-methoxyphenyl)-4,5-diphenyl-1H-imidazol-2-yl)-N,N-diphenylaniline (MID)

The imidazole derivative MID was synthesized by one-pot multicomponent reaction procedure by refluxing the mixture of benzil (0.384 g, 1.82 mmol), 4-methoxyaniline (0.225 g, 1.82 mmol), N,N-diphenylbenzaldehyde (0.5 g, 1.82 mmol), and ammonium acetate (0.985, 12.74 mmol) in acetic acid at 110 °C for 10 h. The resulting crude white solid was washed thoroughly with excess water and dried under vacuum. It was subsequently recrystallized from an ethanol: n-hexane (1:9) to yield a pure off-white solid with 88% yield [11].

Melting Point: 253-254 oC;1H NMR (500 MHz, CDCl3) δ 7.52 (d, 2H, J = 7.3 Hz), 7.25 (d, 2H, J = 8.6 Hz), 7.20 – 7.15 (m, 10H), 7.11 (d, 1H, J = 7.3 Hz), 7.06 (dd, 2H, J = 7.7, 1.8 Hz), 7.01 (d, 4H, J = 7.5 Hz), 6.96 (d, 1H, J = 7.3 Hz), 6.94 – 6.91 (m, 2H), 6.84 (d, 2H, J = 8.8 Hz), 6.70 (d, 2H, J = 8.9 Hz), 3.70 (s, 3H, -OCH3); 13C NMR (126 MHz, CDCl3) δ 158.16 (C-Oaromatic), 146.30(C-Naromatic), 135.06(=Nimidazole), 130.16, 129.81, 128.61, 128.49, 128.27, 127.31, 127.11, 126.88, 126.41, 125.58, 123.90, 122.29, 121.08, 113.21, 54.34 (-OCH3); ESI-MS (m/z) [M+1]: 570 (**Supplementary Info**).

3. Result and discussion

3.1 Chemistry

As illustrated in (**Scheme 1**), the imidazole **(MID)** derivative was designed and prepared to build a donor- π- Acceptor (D-π-A) molecular framework. A extended conjugation system, molecular planarity, and efficient electron delocalization is essential for fluorescent sensors with superior emissive performance. The N,N-diphenyl of aldehyde act as electron-donating moiety, facilitating ICT between donor and acceptor segments, which potentially leads to fluorescence quenching upon coordination with metal ion. The synthesized derivative were thoroughly characterized using ^{1}H-NMR, ^{13}C-NMR and mass spectrometry, as described in the synthesis and spectral analysis sections.

The ^{1}H-NMR spectra of MID showed a singlet at δ 3.70 ppm, attributed to the $-OCH_3$ group, along with 28 aromatic protons distributed across multiple peaks. The ^{13}C-NMR spectra further confirmed the structural feature of each compound. For **MID** the imidazole C=N carbon appeared at 135.06 ppm, the C-N of the aromatic systems at 146.30 ppm and the methoxy carbon at δ 54.34 ppm. The formation of imidazole derivatives was further supported by the electrospray ionization mass spectrometry (ESI-MS), where molecular ion peaks [M+1] was appeared at m/z 570. Overall, the combined spectral data conclusively confirmed the successful synthesis and structural identity of the imidazole derivatives **MID** (**Supplementary Info**).

3.2 Absorption and fluorescence spectral behaviour of imidazole derivatives MID

The imidazole derivatives exhibit a D–π–A framework, attributed to the presence of a stilbene moiety conjugated with the imidazole ring via different linkers: an **N,N-diphenylamine** bridge in MID. This configuration is expected to endow the compounds with intriguing **photo-physical characteristics**. To explore these properties, UV-Vis absorption and fluorescence emission spectra (1 × 10-5 M in acetonitrile) were recorded across various solvents. Solvatochromic behavior was examined to gain insight into the **electronic nature** of the ground and excited states, relaxation mechanisms, variations in Stokes shift, and the typical intramolecular charge transfer (ICT) process [12]. Variations in absorption and emission wavelengths are influenced by solvent polarity, as solvents interact differently with the fluorophores in both electronic states [13]. To elucidate the solvent-dependent optical behavior, absorption spectra were recorded in a range of solvents, including DMF, EtOH, PrOH, CHCl3, DMSO, DCM, CH3CN, dioxane, THF, n-Hexane, and MeOH. Although the influrence of the solvents and surrounding environment on fluorescence spectra is complex, two possible explanation can be proposed: (a) the decrease in emission intensity with polar protic solvent may arise from specific solvent-fluorophore interactions, where polar protic solvents can suppress charge transfer process of MID molecule in the excited state; and (b) solvent molecules may form strong H-bonds with the proton of N-atom in imidazole moiety, thereby hindering intramolecular proton transfer [14].

Variation in UV-visible absorption spectra arises from electronic transitions between ground state and higher excited energy level. The absorption and emission spectra of MID were markedly affected by solvent polarity as depicted in Table 1 and Figure 1a & b.

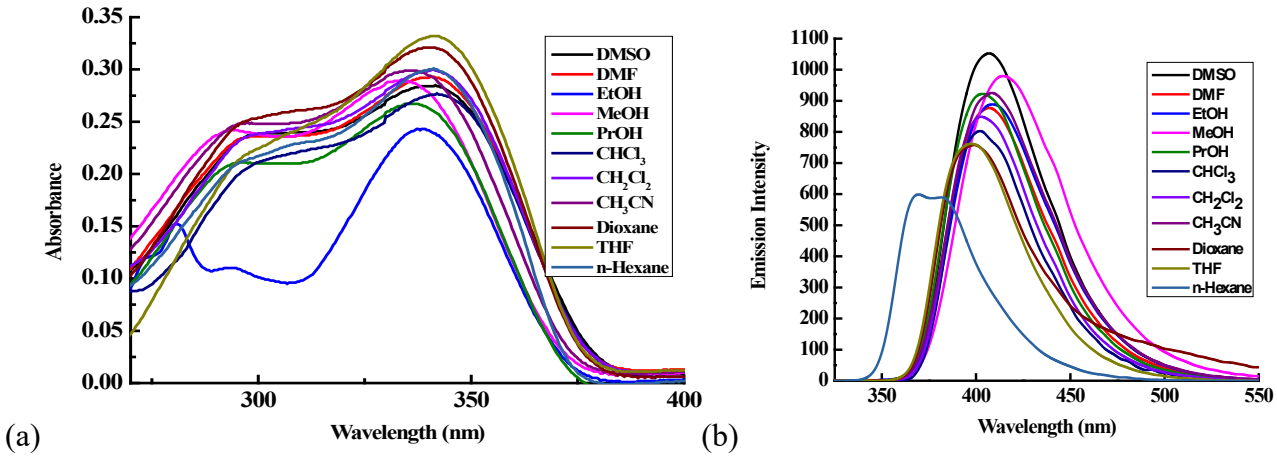

Figure 1. (a) UV-Vis absorbance spectra; (b) fluorescence emission spectra of **MID** (1 x 10^{-5} M) in different solvents.

Table 1. Photo-physical variables and fluorescence quantum efficiency of **MID** in different solvents system.

Solvent	Δf	E_T^N	E_T (30) Kcal mol^{-1}	λ_{ab}(nm)	λ_{em}(nm)	ε $M^{-1}cm^{-1}$	f	μ 12 Debye	$\Delta\nu_{st}$ (cm^{-1})	Φ_f
DMSO	0.263	0.441	45.1	342	408	28400	0.530	6.20	4730	0.34
DMF	0.274	0.404	43.8	341	406	29300	0.550	6.30	4695	0.27
EtOH	0.288	0.654	51.9	339	406	24300	0.473	5.58	4868	0.33
MeOH	0.308	0.762	55.4	334	413	29000	0.664	6.85	5727	0.31
PrOH	0.280	0.520	49.2	337	403	26700	0.519	6.09	4860	0.31
$CHCl_3$	0.148	0.259	39.1	342	402	27700	0.483	5.92	4364	0.26
CH_2Cl_2	0.218	0.472	41.1	341	403	30000	0.541	6.25	4511	0.25
CH_3CN	0.305	0.164	45.6	336	402	29900	0.591	6.49	4948	0.30
Dioxane	0.028	0.210	36.0	340	398	32100	0.550	6.29	4286	0.20
THF	0.208	0.006	35.1	342	399	33200	0.555	6.34	4177	0.21
n-Hexane	0.0002	0.0002	31.1	341	384	30100	0.395	5.34	3284	0.17

The optical properties of the imidazole-based heterocycle were investigated to explore its applicability as a fluorescence sensor for identifying toxic metal ions. Corresponding absorption spectra were recorded at room temperature (25 °C) in a range of solvents [15].

MID displays a modest bathochromic shift of 8 nm in the UV-absorption spectra. Absorbance increased from CH_3CN (336 nm), Hexane (341 nm) to dimethyl sulfoxide (342 nm) as illustrated in (**Table 1 & Figure 1a**). The bathochromic shift was arises due to increased conjugation, π-π* transitions, solvent effects and ICT from diphenylamine donor site of **MID.** Furthermore, the emission spectra of **MID,** excited at 320 nm, displayed a red shift of 29 nm. For **MID**, the emission maxima shifted from 384 nm in hexane to 413 nm in methanol and 408 nm in DMSO. These solvent-induced spectral changes are summarized in (**Tables 1**) and illustrated in (**Figures 1b**). This bathochromic shift was primarily due to π-π* electronic transitions accompanied by photoinduced-ICT in the singlet excited state, and electron donating groups and H-bonding [16].

The molar absorptivity ($\mathcal{E}$) of compounds **MID** exhibited broad absorption bands, indicative of electronic transition from S_1 to S_2 strongly dependent on solvent polarity. The molar absorption coefficient of **MID** decreases on increasing solvent polarity, as shown in (**Table 1**) , this decrease can be attributed to loss of conjugation, solvent effects (such as destabilization of the excited state), or possible aggregation/dimerization in polar solvents. The visual appearance of the imidazole derivatives (1 × 10^{-5} M in AcCN) in different solvents was monitored.

The empirical Dimorth-Reichardt polarity parameters $E_T(30)$ for different solvents was evaluated to examine its relationship with the absorption energy (E_a) and emission energy (E_f) of derivatives **MDI** (**Figure 2).** The evaluation highlight the significant influence of polarity of solvent on photophysical behaviour of derivatives **MID.** A linear correlation between polarity of solvent and the corresponding absorption and emission energies was obtained using (Eq. 1 & 2) [17].

$$E_a = 81.502 - 0.063 \times E_T(30) \quad (1)$$

$$E_f = 66.95 - 0.072 \times E_T(30) \quad (2)$$

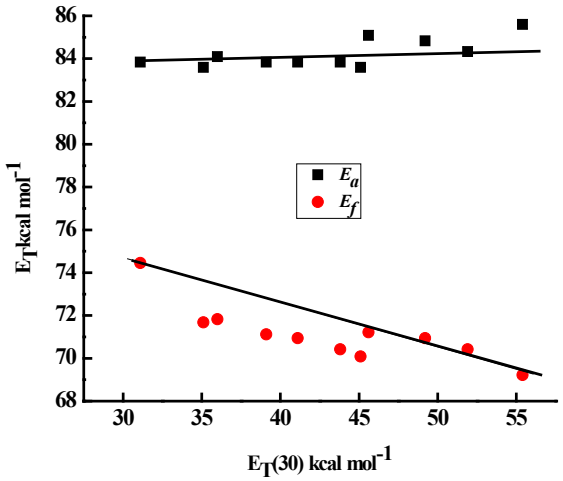

Figure 2: Linear regression plots showing variation in absorption and emission energies (E_a & E_f) with $E_T(30)$ values of various solvents for **MID.**

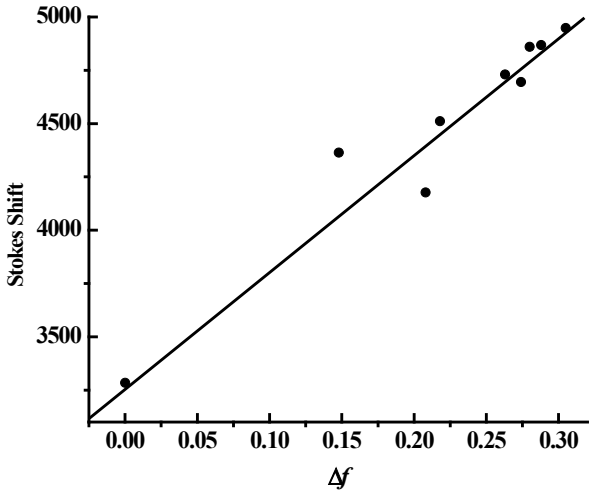

Figure 3. Relationship of Δf versus stokes shift of imidazole derivative (**MID**).

3.3 Evaluation of transition dipole moments, spectral stokes shift and oscillator strength

The physicochemical variables, including Stokes shift ($\Delta\nu_{st}$), transition dipole moments ($\Delta\mu$), and oscillator strength (f), were investigated for the heterocyclic **MID** across different solvents. The change in dipole-moment between the excited and ground state ($\Delta\mu = \mu_e - \mu_g$) was estimated for each derivative in different solvent environments. These key variables were calculated via Lippert-Mataga Eq. (3). Furthermore, the Δf of the solvents was derived utilizing Eq. (4). A linear relationship between orientation polarizability (Δf) and $\Delta\nu_{st}$ (**Figure 3**) suggests that the $\Delta\nu_{st}$ is significantly influenced by polarity of solvent or dielectric response. By using Lippert-Mataga Eq. (3) and the calculated ground (μ_g) and excited state dipole moments

$$\Delta\bar{\nu}_{st} = \nu_{abs} - \nu_{em} = \frac{2\Delta\mu^2}{hca^3}\Delta f + Const.$$

(μ_e), the Onsager cavity radius (a) for the imidazole derivatives **MID** was determined using Eq. (5) [18].

(3)

$$\Delta f = \frac{\varepsilon - 1}{2\varepsilon + 1} - \frac{\eta^2 - 1}{2\eta^2 + 1}$$

(4)

$$a = \left(\frac{3M}{4N\pi d}\right)^{1/3}$$

(5)

The transition dipole moments for the heterocyclic imidazole **MDI** in various solvents were determined employing Eq. (6) [19]. Moreover, the oscillator strengths of the **MID** in different solvents were evaluated by Eq. (7) [20].

$$\mu^2 = \frac{f}{4.72\times10^{-7}\,E_{max}}$$

(6)

$$f = 4.32\times10^{-9}\int\varepsilon(\bar{\nu})\,d\bar{\nu}$$

(7)

3.4 Quantum emission efficiencies of imidazole derivatives across various solvents.

The fluorescence quantum efficiency (ϕ_f) is a crucial photophysical parameter that indicates the efficiency with which a molecule converts absorbed light into emitted fluorescence. In this study, the quantum yields of the imidazole derivatives **MID** was evaluated in various solvents using the relative method, with fluorescein in ethanol (ϕ_r = 0.95) serving as the reference standard. The quantum yield was calculated using Equation (8) [21].

$$\Phi_f = \Phi_r \frac{I \times A_r \times \eta^2}{I_r \times A_r \times \eta_r^2} \qquad (8)$$

The quantum yields of **MID** was found to be solvent-dependent, primarily affected by solvent polarity, H-bond donor ability, and electronic polarizability. As shown in (**Table 1**), an increase in solvent polarity generally led to higher quantum yield values, particularly in polar aprotic solvents such as DMSO and $CHCl_3$. For instance, ϕ_f increased from 0.17 in hexane to 0.34 in chloroform for **MID**. These enhancements are attributed to increased charge transfer efficiency, facilitated by solvent–solute interactions and conformational flexibility. Nevertheless, in polar protic solvents like methanol and ethanol, a decrease in quantum yield was observed. This reduction is associated with positive solvatokinetic effects, where hydrogen bonding with proton-donor solvents promotes non-radiative decay pathways, thereby lowering fluorescence efficiency. The electron-donating substituents on **MID** is N,N-diphenyl groups also play a role in modulating the quantum yield via intramolecular charge transfer (ICT) interactions with solvents.

The trend of quantum yield variation with solvent polarity was further analyzed using Reichardt's solvent polarity parameter ($E_T(30)$). The plots of ϕ_f against $E_T(30)$ (**Figure 4**) revealed a strong correlation, reinforcing the prominent role of the solvent environment in governing the photo-physical properties of these imidazole derivatives. Overall, the results demonstrate that **MID** exhibited distinct solvent-dependent fluorescence behaviours, making them sensitive probes for exploring solvent polarity effects.

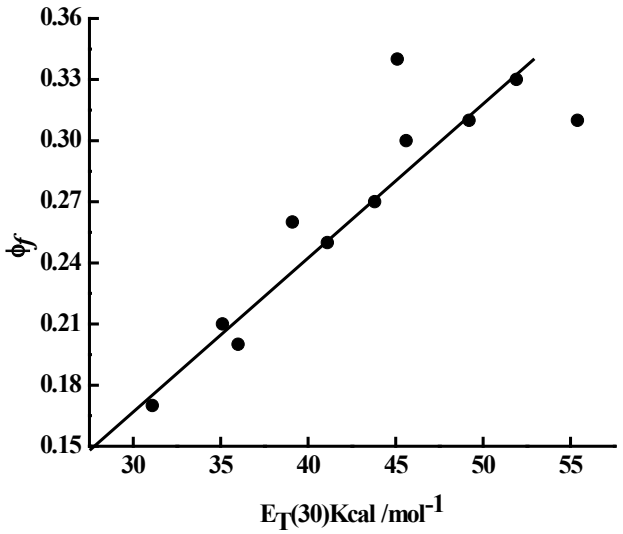

Figure 4. Correlation plots of ϕ_f versus $E_T(30)$ for imidazole derivaitves (**MID**).

3.5 Fluorescent sensing behavior of MID for metal ion detection

The influence of different cation (Na^+, Mg^{2+}, Ag^+, Ca^{2+}, Zn^{2+}, Mn^{2+}, Co^{2+}, Al^{3+}, Cu^{2+}, Pb^{2+}, Cd^{2+}, Hg^{2+}, Fe^{2+}, Fe^{3+}, and Ce^{4+} ions), which are significant in biological and environmental contexts, was evaluated using newly synthesized imidazole-based sensors **MID** through fluorescence emission studies acetonitrile (1×10^{-5} M) solution. The excitation wavelengths were optimized in the range of 320 nm for **MID** to achieve maximum fluorescence intensity for each imidazole derivative. The spectroscopic responses of the **MID** toward various cations were investigated in CH_3CN-H_2O solution (pH 7.4, CH_3CN:H_2O; 9:1; v/v) at ambient temperature. These studies aimed to assess the selectivity and sensitivity of the newly developed sensors toward biologically and ecologically relevant metal ions.

The fluorescence titration of sensor with different metal ion was conducted and found that compound **MID** exhibited fluorescence emission upon excitation at 320 nm, and showing strong emission intensity with a longer wavelength between the ranges of 350-625 nm. Except of mercury ion (Hg^{2+}), other competing cations, such as Na^+, Mg^{2+}, Ag^+, Ca^{2+}, Zn^{2+}, Mn^{2+}, Co^{2+}, Al^{3+}, Cu^{2+}, Pb^{2+}, Cd^{2+}, Fe^{2+}, Fe^{3+}, and Ce^{4+} ions (each at 5.0 equiv.) did not cause significant changes in the emission spectra. The **MID** alone displayed a strong emission intensity peak at 409 nm; however, upon the incorporation of Hg^{2+} ion (5.0 equiv.) a dramatic quenching of emission (~ 25 folds) was displayed, as well as bathochromic shift in the emission maximum from 409 nm to 532 nm, as shown in **Figure 5.** These changes attributed to the complexation of **MID** + Hg^{2+} ion, likely because of photo-induced electron transfer (PET), enhanced π-conjugation and hydrogen bonding. These results suggest that **MID** could function as a fluorescent sensor for the selective identification of Hg^{2+} ions, as depicted in the **Figure 5.**

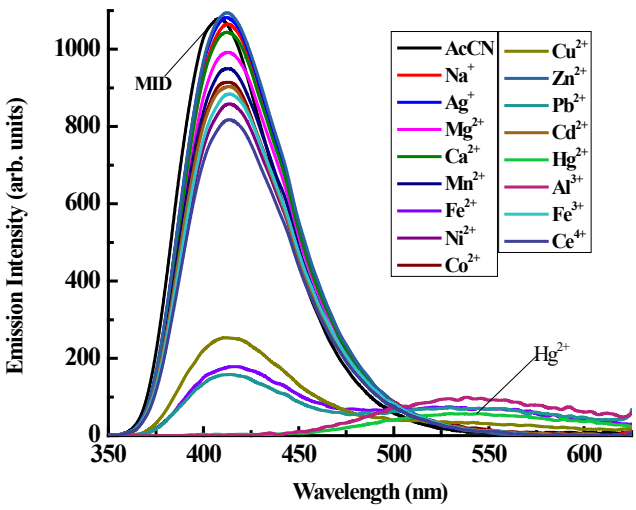

Figure 5. Fluorescence emission spectra of **MID** (1.0×10^{-5} M) recorded after the addition of various metal ions (5.0×10^{-4} M) Na^+, Mg^{2+}, Ag^+, Ca^{2+}, Zn^{2+}, Mn^{2+}, Co^{2+}, Al^{3+}, Cu^{2+}, Pb^{2+}, Cd^{2+}, Hg^{2+}, Fe^{2+}, Fe^{3+}, and Ce^{4+} ions in a CH_3CN/ water (9:1, v/v).

The sensing behaviour of imidazole derivatives **MID** towards various concentrations ($0.1\text{-}0.9 \times 10^{-4}$ M) of metal ions was systematically investigated using fluorescence titration studies. With incremental addition of metal ions, a gradual quenching of fluorescence emission was observed at 546 nm for **MID**. This quenching exhibited a strong linear correlation with the increasing concentrations of Hg^{2+} suggesting efficient and selective sensing behaviour. The electron-donating N,N-benzyl groups present in **MID** facilitate electron transfer towards the aldehyde group of imidazole ring, forming a strong push–pull electronic system that enhances metal ion interaction. The Figure 6 depict the excellent linearity with correlation coefficients (R^2) of 0.9935 **MID**- Hg^{2+}. These results establish **MID** as highly selective turn-Off fluorescent chemosensors for the recognition of Hg^{2+} ions.

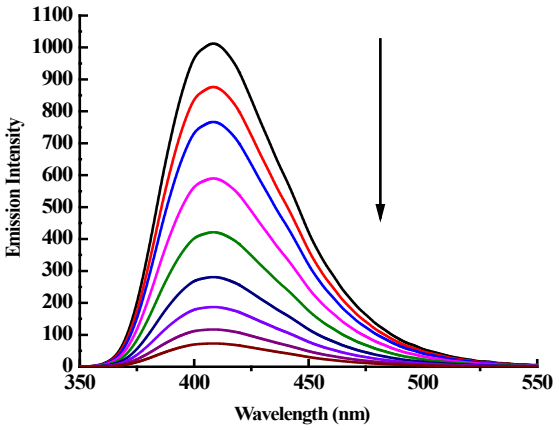

Figure 6: Fluorescence spectra of MID at different concentration of Hg2+ ion

A **Job's plot technique** was employed to investigate the **stoichiometry ratio** between imidazole derivatives MID and mercury (II) ion as shown in (Figure 7). Subsequently, fluorescence titration experiments were conducted by varying the concentrations of these metal ions (1–9 × 10-3 M) in an **CH3CN:H2O mixture (9:1, v/v)**, while maintaining the total concentration of each imidazole derivative at **1 × 10-5 M**. The resulting emission spectra (Figure 7) were analysed to evaluate the coordination stoichiometry of the sensor–metal ion complexes. The titration profiles revealed a **progressive**

quenching of fluorescence intensity upon the incremental addition of Hg2+ ions, indicating strong interactions with the metal ions. The maximum quenching occurred when the mole fraction of Hg2+ reached approximately **0.61,** as depicted in (**Figure 7**). These values strongly suggest a **2:1 binding stoichiometry ratio** between the imidazole ligands and the corresponding metal ions (Scheme 2).

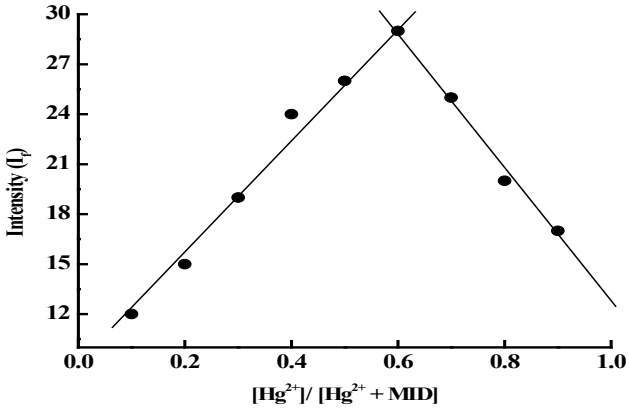

Figure 7: Job's plot illustrating Fluorescence Intensity vs. mole fraction of **MID** with Hg^{2+} ions.

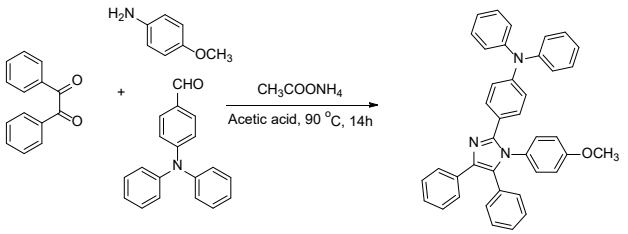

Scheme 1: Schematic representation of one-pot synthesis of imidazole derivative (MID)

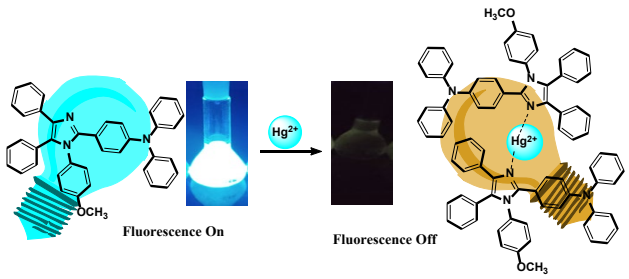

Scheme 2: Schematic structure of coordination interaction between MID and Hg^{2+} ions (2:1).

Conclusion

In summary, a highly fluorescent and sensitive imidazole-based probe **MID** was successfully synthesized for the recognition of Hg^{2+} ion in environmental samples. The senor MID displayed a pronounced turn-Off fluorescence behaviours upon interaction with mercury(II) ions, enabling the recognition of very low concentrations of mercury. The molecular structure of **MID** was characterized by ^{1}H-NMR, ^{13}C-NMR and mass spectrometry. The interaction and complexation behaviour between MID and Hg^{2+} ions were further investigated using Job's plot analysis, which revealed 2:1 binding stoichiometry (MID:Hg^{2+}). Furthermore, the probe demonstrated a rapid response and excellent selectivity towards Hg^{2+} ions, highlighting its potential application for the sensitive and selective recognition of Hg^{2+} ions in real environmental samples.

Supplementary Information

Reference

[1] Guo Y, An J, Tang H, Peng M, Suzenet F. Selective and "turn-off" fluorimetric detection of mercury (II) based on coumarinyldithiolane and coumarinyldithiane in aqueous solution. Materials Research Bulletin. 2015 Mar 1;63:155-63.

[2] Bozkurt E, Gul HI. A novel pyrazoline-based fluorometric "turn-off" sensing for Hg2+. Sensors and Actuators B: Chemical. 2018 Feb 1;255:814-25.

[3] Vengaian KM, Britto CD, Sekar K, Sivaraman G, Singaravadivel S. Phenothiazine-diaminomalenonitrile based colorimetric and fluorescence "turn-off-on" sensing of Hg2+ and S2−. Sensors and Actuators B: Chemical. 2016 Nov 1;235:232-40.

[4] Patil SK, Das D. A nanomolar detection of mercury (II) ion by a chemodosimetric rhodamine-based sensor in an aqueous medium: Potential applications in real water samples and as paper strips. Spectrochimica Acta Part A: Molecular and Biomolecular Spectroscopy. 2019 Mar 5;210:44-51.

[5] Xu X, Li YF, Zhao J, Li Y, Lin J, Li B, Gao Y, Chen C. Nanomaterial-based approaches for the detection and speciation of mercury. Analyst. 2015;140(23):7841-53.

[6] Wang Z, Zhang Y, Yin J, Yang Y, Luo H, Song J, Xu X, Wang S. A novel camphor-based "turn-on" fluorescent probe with high specificity and sensitivity for sensing mercury (II) in aqueous medium and its bioimaging application. ACS Sustainable Chemistry & Engineering. 2020 Jul 29;8(33):12348-59.

[7] Chatterjee A, Banerjee M, Khandare DG, Gawas RU, Mascarenhas SC, Ganguly A, Gupta R, Joshi H. Aggregation-induced emission-based chemodosimeter approach for selective sensing and imaging of Hg (II) and methylmercury species. Analytical chemistry. 2017 Dec 5;89(23):12698-704.

[8] Singh A, Kaur S, Singh N, Kaur N. Fluorometric sensing of Hg 2+ ions in aqueous medium by nano-aggregates of a tripodal receptor. Organic & Biomolecular Chemistry. 2014;12(14):2302-9.

[9] Hu J, Li J, Qi J, Sun Y. Selective colorimetric and "turn-on" fluorimetric detection of cyanide using an acylhydrazone sensor in aqueous media. New Journal of Chemistry. 2015;39(5):4041-6.

[10] Jawad SH, Al-Adilee KJ. Synthesis and characterization of a new 1-methyl imidazole derived ligand with its ionic complexes Pd (II) and Pt (IV) and study of biological activity as anticancer and antioxidant. Results in Chemistry. 2022 Jan 1;4:100573.

[11] Krishnan U, Manickam S, Iyer SK. Turn-off fluorescence of imidazole-based sensor probe for mercury ions. Sensors & Diagnostics. 2024;3(1):87-94.

[12] Palion-Gazda J, Machura B, Klemens T, Szlapa-Kula A, Krompiec S, Siwy M, Janeczek H, Schab-Balcerzak E, Grzelak J, Maćkowski S. Structure-dependent and environment-responsive optical properties of the trisheterocyclic systems with electron donating amino groups. Dyes and Pigments. 2019 Jul 1;166:283-300.

[13] Haidekker MA, Brady TP, Lichlyter D, Theodorakis EA. Effects of solvent polarity and solvent viscosity on the fluorescent properties of molecular rotors and related probes. Bioorganic chemistry. 2005 Dec 1;33(6):415-25.

[14] Li XG, Liao Y, Huang MR, Strong V, Kaner RB. Ultra-sensitive chemosensors for Fe (III) and explosives based on highly fluorescent oligofluoranthene. Chemical Science. 2013;4(5):1970-8.

[15] E. Morgan. *Vogel's textbook of practical organic chemistry. 5th edn. Endeavour, 14(3),* (1990) *148*. doi:10.1016/0160-9327(90)90017-l.

[16] Khopkar S, Jachak M, Shankarling G. Novel A2-D-A1-D-A2 type NIR absorbing symmetrical squaraines based on 2, 3, 3, 8-tetramethyl-3H-pyrrolo [3, 2-h] quinoline: Synthesis, photophysical, electrochemical, thermal properties and photostability study. Spectrochimica Acta Part A: Molecular and Biomolecular Spectroscopy. 2019 Mar 15;211:114-24.

[17] Yin SY, Sun SS, Pan M, Chen L, Wang Z, Hou YJ, Fan YN, Wang HP, Su CY. An imidazole based ESIPT molecule for fluorescent detection of explosives. Journal of Photochemistry and Photobiology A: Chemistry. 2018 Mar 15;355:377-81.

[18] Nandy R, Sankararaman S. Donor-acceptor substituted phenylethynyltriphenylenes–excited state intramolecular charge transfer, solvatochromic absorption and fluorescence emission. Beilstein journal of organic chemistry. 2010 Oct 18;6(1):992-1001.

[19] Sıdır YG, Sıdır İ. Solvatochromic fluorescence of 4-alkoxybenzoic acid liquid crystals: ground and excited state dipole moments of monomer and dimer structures determined by solvatochromic shift methods. Journal of Molecular Liquids. 2015 Nov 1;211:591-603.

[20] Iliashenko RY, Borodin OO, Wera M, Doroshenko AO. 2, 5-bis [2-(2-phenyl-1, 3-oxazol-5-yl) phenyl]-1, 3, 4-oxadiazole–new sterically hindered high Stokes shift fluorophore sensitive to media viscosity. Journal of Photochemistry and Photobiology A: Chemistry. 2015 Feb 1;298:68-77.

[21] Chen H, Fang S, Wang L, Liu X, Yan J, Zhang N, Zheng K. Tetraphenylene-chalcone hybrid derivatives: Synthesis, structural, fluorescence properties and imaging in living cells. Journal of Molecular Liquids. 2021 Jan 1;321:114913.